Innovative Efficient Element for Analysis of FGM Plates Using FEM

Shahnavaz, F.[1] , Attarnejad, R.[2]* , Shaloudegi, K.[3] and Kazemi Firouzjaei, R.[4]

[1] M.Sc., Researcher, School of Civil Engineering, College of Engineering, University of Tehran, Tehran, Iran.
[2] Professor, School of Civil Engineering, College of Engineering, University of Tehran, Tehran, Iran.
[3] M.Sc., Researcher, School of Civil Engineering, Clarkson, Potsdam, USA.
[4] M.Sc., Researcher, School of Civil Engineering, Polytechnic University of Catalonia (UPC), Barcelona, Spain.

ABSTRACT: In order to obtain accurate results from displacement-based Finite Element Method (FEM), it is crucial to introduce accurate shape functions that interpolate the displacement field within an element. This paper attempts to provide such a new component by using Finite Element method using Basic Displacement Function (BDFs) for the free vibration analysis of plates with in-plane Functionally Graded Material (FGM). The first step is to introduce displacement functions and compute them using the energy method. Later, new shape functions are developed based on stiffness and force methods used to model the mechanical behavior of the element, wherein the shape functions benefit from the generality and accuracy of the stiffness and force methods. Last, the plate is analyzed using Finite Element method to derive the structural matrices from new shape functions. Several numerical examples demonstrate the accuracy and efficiency of the method, and a special material graded index named Ns is introduced.

Keywords: Basic Displacement Functions (BDFs), Finite Element Method (FEM), Free Vibration, Functionally Graded Materials (FGMs), Kirchhoff-Love Plate Theory.

1. Introduction

There are many applications of thin rectangular plates in modern engineering, such as in civil engineering, mechanical engineering, marine industry, and aeronautical engineering. (Hamrit and Necib, 2018). Over the last century, many research studies have been conducted on plates. A mathematical model of the membrane theory of plates was first presented by Euler in the eighteenth century (Naumenko and Eremeyev, 2017). In later years, Lagrange devised differential equations to describe plate free vibrations (Ramkumar et al., 1987). Over the years, a great deal of investigation has been conducted on the dynamic analysis of thin plates (Wang et al., 2017) as well as dynamic analyses of variable thickness plates such as sandwich panels (Vatani Oskouei and Kiakojouri, 2015). Leissa provides a thorough documentation of many of them (Leissa, 1969). The Kirchhoff

---

* Corresponding author E-mail: Attarnjd@ut.ac.ir

hypothesis dictates that thin plates will vibrate as a result of their classical vibration behavior. The use of structural elements with variable thickness reduces the weight of structure elements and improves material utilization, resulting in more economic design of structures. Static and stability analysis is an essential component of the design of these structures (Tenenbaum et al., 2020).

Material properties of Functionally Graded Materials (FGMs) are continuously variable according to spatial coordinates. FGMs display gradual variations in material properties, unlike laminated composites that can suffer from interfacial stresses leading to delamination and crack propagation (Das, 2010). Changing the thickness direction or changing the in-plane material can be used to achieve this. Initially, the idea of FGMs was proposed by Bever and Shen (1997) to produce polymer (Bever. Since there is no blunt conversion in material properties across the confluence of dissimilar materials, FGMs avoid problems associated with conventional composites, such as large inter-laminar stresses, crack initiation, and delamination (Gupta, 2020). Afterward application of FGMs noteworthy increased in aerospace engineering and micro-electrical industry. Since the mid-1990s, FGMs have been applied in many fields, such as optics, human implants, engine components, turbine blades, and many others. Researchers have also given these FGMs considerable attention (Miyamoto et al., 1999). According to the wide application of FGMs, the behavior of FGM structures has been studied in several studies such as beams, plates, and shells (Vidal et al., 2021). However, most of these studies deal with FGMs with material indices changing in thickness direction merely (Njim et al., 2021).

In recent years, many researchers have investigated the static and dynamic analyses of plates with different plate theories in conjunction with the study of their material property variation. For example, the static analysis of functionally graded rectangular plates using third-order shear deformation theory was presented by Reddy (2000). Based on Reddy's theory, Cheng and Batra (2000) investigated the identical eigenvalues between the functionally graded plates and those of membranes subjected to uniform in-plane loads. They also related the deflection of FGM plates predicted by the first-order and the third-order shear deformation theory to that of an substitute compatible Kirchhoff plate. Moreover, several studies have been done on bi-directional FGM beams (Şimşek, 2016). Among them, Goupee and Vel (2006) developed a methodology for the simulation and optimization of the vibration response of bi-directional functionally graded beams. To the best of the author's knowledge, there are a few papers in the literature that have considered the in-plane material inhomogeneity. For instance, Liu et al. (2010) presented the free vibration of FGM plates with in-plane material inhomogeneity and obtained a Levy-type solution in the specific case where the plate is merely supported alongside to the material gradient direction. In addition, an elastoplastic Mindlin-Reissner plate is analyzed using a non-layered Finite Volume formulation (Fallah et al., 2017). Recently, with the inclusion of porosity, free vibration analysis was carried out on tapered Functionally Graded Material (FGM) plates (Kumar et al., 2021). Numerical method is also used to analyse the performance of walls (Shahir and Delfan, 2021). Based on modal strain energy and Dempster-Shafer evidence theory, a damage detection method is presented for finding damage in two-layer grids using only a few mode shapes (Teimouri et al., 2021). An asymptotic framework for layered plates is developed with piecewise uniform problem parameters. As well as functionally graded shells, coatings and interfacial layers, it allows various extensions (Kaplunov et al., 2021). A two-parameter model of Winkler-Pasternak's elastic medium with Aluminum

and Alumina porosity is used to model the interaction between FGM plate and elastic foundation (Saidi and Sahla, 2019). Considering porosities that may occur inside functionally graded materials (FGMs) during their fabrication, a higher-order shear deformation model is developed for static and free vibration analyses of functionally graded beams (Hadji et al., 2019). Also, the nonlinear bending of functionally graded (FG) circular sector plates has been investigated when they are subjected to transverse mechanical loading (Fallah and Karimi, 2019).

In the case of general variations of the material and geometry of the plate, there is no closed-form solution, so alternative numerical techniques are required, e.g. the Rayleigh-Ritz method (Kumar, 2018), Differential Quadrature Method (DQM) (Bacciocchi et al., 2016), Differential Least-Square-based Finite Difference (LSFD) (Liu et al., 2021), Differential Quadrature Element Method (DQEM) (Makvandi et al., 2019), Transformed Differential Quadrature Method (TDQM) (Malekzadeh, 2018), generalized differential quadrature rule (Lal and Siani, 2020), methods based on the Green Functions (Mora et al., 2016), 2D Differential Transform Method (2D-DTM) (Chiba, 2019). FEM is one of these techniques.

The goal of this paper is to present an effective tool for analyzing plates with in-plane Functionally Graded Materials (FGMs) using the FEM. A unit load method is used to derive Basic Displacement Functions (BDFs). Afterward, in terms of BDFs, new shape functions have been derived from a mechanical perspective. The Finite Element method is finally used in order to derive structural stiffness and a consistent mass matrix for the in-plane FGM plate. The present method has been illustrated using numerical examples and graphs to illustrate both its accuracy and economy. Moreover, a special material graded index has been presented, namely *Ns*. This method is really efficient for analyzing FGM plates and makes it possible to do a Finite Element analysis with lower segments. Thus, it will result to have the answers more quickly on a medium computer.

2. Materials and Methods

A general case is considered in this study. In Figure 1, a rectangular FGM plate with length *a* and width *b* is shown in a Cartesian coordinate system. Also, $h(x,y)=h_0 \times H(x) \times H(y)$: is the variable thickness of the plate, where h_0: is plate thickness at the coordinate center, and $H(x)$ and $H(y)$: stand for thickness abnormality along *x* and *y* directions, respectively. Figure 2 depicts positive signs for the shear forces and bending moments. The material properties, such as the elastic modulus, *E* and mass density, ρ are varying in-plane as follows:

$$E = V_l E_l + V_r E_r \tag{1}$$

$$\rho = V_l \rho_l + V_r \rho_r \tag{2}$$

in which:

$$V_l + V_r = 1 \tag{3}$$

where V_l and V_r: are the volumes of fraction in the left and right sides of the plate along the direction with material inhomogeneity which *y* : is the direction in this study.

In order to understand Kirchhoff-Love plate theory, the following assumptions has been made (Szilard, 2004):
1. z is not affected by displacement along z-direction;
2. Before deformation, portions of the plate that were parallel to its middle surface remain parallel to it after deflection;
3. Deformation due to shear is ignored;
4. The deflections and rotations of plates are small compared to their dimensions;
5. Transverse stresses in the plate surface direction can be ignored.

As a result of Kirchhoff-Love plate theory, the following relationships can be written as follows.
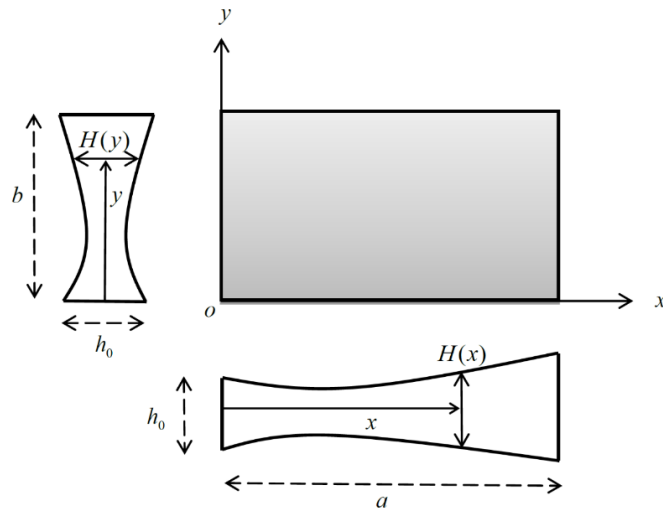
Fig. 1. FGM rectangular plate in a Cartesian coordinate system
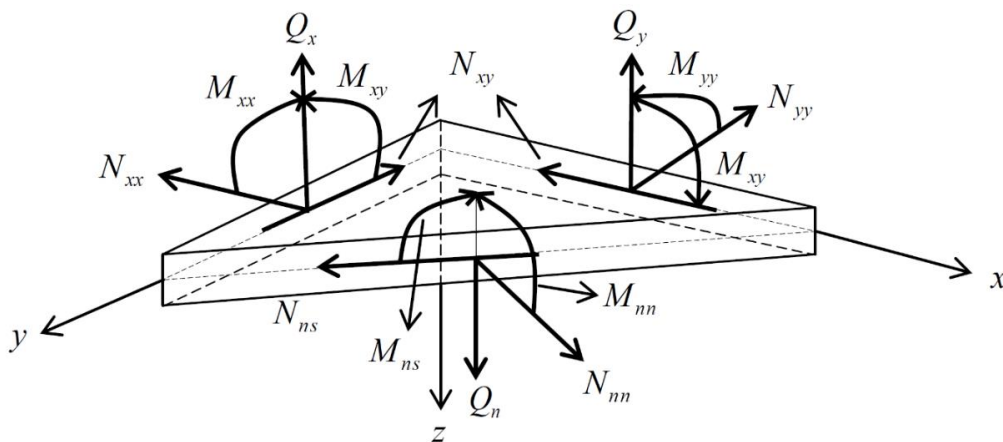
Fig. 2. Positive sign conventions for shear forces and bending moments

Deranication in x, y and z directions are given as:

$$u_x = -z\theta_x = -z\frac{\partial w_0}{\partial x},$$

$$u_y = -z\theta_y = -z\frac{\partial w_0}{\partial y}, \quad u_z = w_0 \qquad (4)$$

where θ_x and θ_y: stand for bending rotations about x and y axis, respectively, in the following manner:

$$\theta_x = \frac{\partial w_0}{\partial x}, \qquad \theta_y = \frac{\partial w_0}{\partial y} \qquad (5)$$

and w_0: is the displacement function. Strain/displacement relations give:

$$\varepsilon_{xx} = -z\frac{\partial^2 w_0}{\partial x^2}, \quad \varepsilon_{yy} = -z\frac{\partial^2 w_0}{\partial y^2},$$

$$\varepsilon_{xy} = -2z\frac{\partial^2 w_0}{\partial x \partial y}, \quad \varepsilon_{xz} = \varepsilon_{yz} = \varepsilon_{zz} = 0 \qquad (6)$$

Constitutive equations give:

$$\sigma_{xx} = \frac{E}{1-v^2}(\varepsilon_{xx} + v\varepsilon_{yy}) = \frac{-Ez}{1-v^2}(\frac{\partial^2 w_0}{\partial x^2} + v\frac{\partial^2 w_0}{\partial y^2}) \qquad (7)$$

$$\sigma_{yy} = \frac{E}{1-v^2}(\varepsilon_{yy} + v\varepsilon_{xx}) = \frac{-Ez}{1-v^2}(\frac{\partial^2 w_0}{\partial y^2} + v\frac{\partial^2 w_0}{\partial x^2}) \qquad (8)$$

$$\sigma_{xy} = \frac{E}{1-v^2}(\frac{1-v}{2}\varepsilon_{xy}) = \frac{-Ez}{1+v}(\frac{\partial^2 w_0}{\partial x \partial y}) \qquad (9)$$

Applying Eqs. (7) to (9), moments per unit length are represented by

$$M_{xx} = \int_{-h/2}^{h/2} z\,\sigma_{xx}dz = -D(\frac{\partial^2 w_0}{\partial x^2} + v\frac{\partial^2 w_0}{\partial y^2}) \qquad (10)$$

$$M_{yy} = \int_{-h/2}^{h/2} z\,\sigma_{yy}dz = -D(\frac{\partial^2 w_0}{\partial x^2} + v\frac{\partial^2 w_0}{\partial y^2}) \qquad (11)$$

$$M_{xy} = \int_{-h/2}^{h/2} z\,\sigma_{xy}dz = -D(1-v)(\frac{\partial^2 w_0}{\partial x \partial y}) \qquad (12)$$

where $D = \frac{E}{12(1-v^2)}h(x,y)^3$: is the bending rigidity of the plate and v: is Poisson's ratio which is consistent.

Based on a harmonic abnormality of $w_0(x,y,t)$ as the transverse displacement of the FGM plate, Eq. (13) can be written.

$$w_0(x,y,t) = w(x,y)e^{i\omega t} \qquad (13)$$

where ω: denotes natural frequency. FGM variable thickness thin plates obey the following differential equation (Van Vinh et al., 2021):

$$\frac{\partial^2}{\partial x^2}\left[-D\left(\frac{\partial^2 w}{\partial x^2} + v\frac{\partial^2 w}{\partial y^2}\right)\right]$$
$$+ 2\frac{\partial^2 w_0}{\partial x\partial y}\left[-D(1-v)\left(\frac{\partial^2 w}{\partial x\partial y}\right)\right]$$
$$+ \frac{\partial^2}{\partial y^2}\left[-D\left(\frac{\partial^2 w}{\partial y^2} + v\frac{\partial^2 w}{\partial yx^2}\right)\right]$$
$$= -\rho h w\omega^2 + \frac{\rho h^3 \omega^2}{12}\left(\frac{\partial^2 w}{\partial x^2} + \frac{\partial^2 w}{\partial y^2}\right)$$

(14)

2.1. BDFs Definition

Various types of beams have been used in different ways with Basic Displacement Functions (BDFs) (Attarnejad et al., 2010). It discusses how to calculate BDFs for tapered FGM plates, followed by a discussion of their applications in deriving nodal flexibility matrices.

Pachenari and Attarnejad (2014a) interpreted BDFs to be the nodal displacements of FGM plates whose boundary conditions are Clamped-Clamped-Free-Free (C-C-F-F). Since it has only one free node and other conditions derived from it, they assumed this condition. An element's x- or y-axis transverse displacement or rotation angle is the result of a unit load acting at x- or y-distance. It is possible to specify detail BDFs for node i as below (the edges adjacent to node i are free, whereas the edges adjacent to the other are clamped):

b_{wi}: is load acting at x, y causes a transverse displacement of node i (Figure 3a); $b_{\theta xi}$: is a unit load acting at x, y bends rotation of node i in the x-direction (Figure 3b); $b_{\theta yi}$: is a unit load acting at x, y bends the rotation of node i in the y-direction (Figure 3c). nodes $i = 1, 2, 3$ and 4 are respectively shown in Figure 3. The reciprocal theorem is applied to all the BDFs in order to determine their equivalent systems. BDFs are the transverse displacements of an element due to a unit nodal load or moment. An arbitrary point (such as point(x, y)) on the element is considered. As a result, BDFs in node i are equivalent since edges that end at node i are free, but others are clamped:
b_{wi}: is an acting unit load at node i causes transverse displacement at distances x and y (Figure 4a); $b_{\theta xi}$: is an x-directed moment acting on node i for distance x and y will result in a transverse displacement at distances x and y; $b_{\theta yi}$: is the y-axis motion of the unit moment at node i at distances x and y is the result of transverse displacement at distances x and y (Figure 4c).

2.2. Nodal Flexibility Matrices

According to the concept of equivalent definitions of BDFs, nodal flexibility matrices can be derived for node i of the FGM plate element.

On the basis of the equivalent definitions of BDFs and its first derivative, nodal flexibility matrices can be determined for all nodes in terms of BDFs:
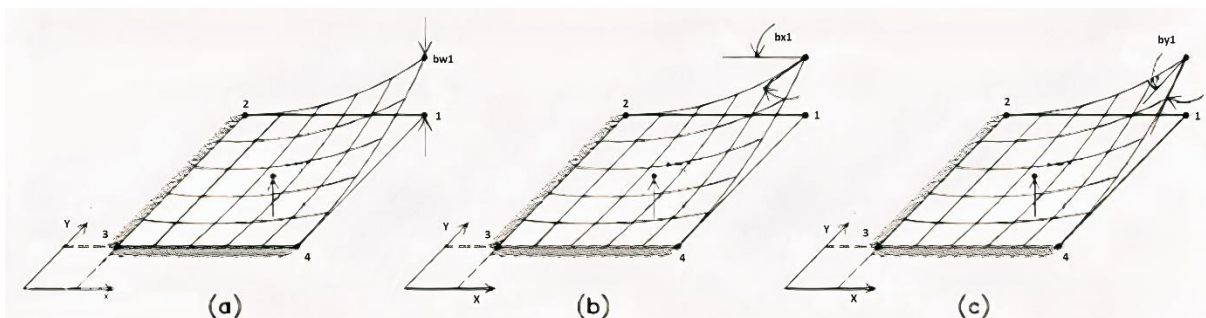
Fig. 3. The transverse displacements of an arbitrary point due to a unit nodal load: a) Load acting at x, y causes a transverse displacement of node; b) Unit load acting at x, y bends rotation of node 1 in the x-direction; and c) unit load acting at x, y bends the rotation of node 1 in the y-direction

$$F_{ii} = \begin{bmatrix} \dfrac{db_{wi(x,y)}}{dx}|_{xi,yi} & \dfrac{db_{\theta xi(x,y)}}{dx}|_{xi,yi} & \dfrac{db_{\theta yi(x,y)}}{dx}|_{xi,yi} \\ \dfrac{db_{wi(x,y)}}{dy}|_{xi,yi} & \dfrac{db_{\theta xi(x,y)}}{dy}|_{xi,yi} & \dfrac{db_{\theta yi(x,y)}}{dy}|_{xi,yi} \end{bmatrix}$$

By multiplication of flexibility matrix and force matrix, the displacement of each node obtains.

2.3. BDFs Computation

BDFs can be calculated for each node using methods based on energy because they contain pure mechanical essence. In this study the unit load method (virtual work) is employed as follow (Zakeri et al., 2016):

Node 1:

$$b_{w1(x,y)}$$
$$= \frac{1}{m} \int_{\beta B}^{y} \int_{\alpha A}^{x} \frac{(A-s)(x-s)}{s^{3r}t^{3l}} \left(\frac{x-A}{k}\right)^c \left(\frac{y-B}{j}\right)^d dsdt$$
$$+ \frac{1}{m} \int_{\beta B}^{y} \int_{\alpha A}^{x} \frac{(B-t)(y-t)}{s^{3r}t^{3l}} \left(\frac{x-A}{k}\right)^c \left(\frac{y-B}{j}\right)^d dsdt$$

$$b_{\theta 1(x,y)} = \frac{1}{m} \int_{\beta B}^{y} \int_{\alpha A}^{x} \frac{(x-s)}{s^{3r}t^{3l}} (\frac{x-A}{k})^c (\frac{y-B}{j})^d dsdt$$

$$b_{\theta 1(x,y)} = \frac{1}{m} \int_{\beta B}^{y} \int_{\alpha A}^{x} \frac{(y-t)}{s^{3r}t^{3l}} (\frac{x-A}{k})^c (\frac{y-B}{j})^d dsdt$$

Node 2:

$$b_{w2(x,y)}$$
$$= \frac{1}{m} \int_{\beta B}^{y} \int_{x}^{A} \frac{s(x-s)}{s^{3r}t^{3l}} \left(\frac{x-A}{k}\right)^c \left(\frac{y-B}{j}\right)^d dsdt$$
$$+ \frac{1}{m} \int_{\beta B}^{y} \int_{\alpha A}^{x} \frac{(B-t)(y-t)}{s^{3r}t^{3l}} \left(\frac{x-A}{k}\right)^c \left(\frac{y-B}{j}\right)^d dsdt$$

$$b_{\theta x2(x,y)}$$
$$= \frac{1}{m} \int_{\beta B}^{y} \int_{\alpha A}^{x} \frac{(x-s)}{s^{3r}t^{3l}} (\frac{x-A}{k})^c (\frac{y-B}{j})^d dsdt$$

$$b_{\theta y2(x,y)}$$
$$= \frac{1}{m} \int_{\beta B}^{y} \int_{x}^{A} \frac{(y-t)}{s^{3r}t^{3l}} (\frac{x-A}{k})^c (\frac{y-B}{j})^d dsdt$$

Node 3:

$$b_{w3(x,y)}$$
$$= \frac{1}{m} \int_{y}^{B} \int_{x}^{A} \frac{s(x-s)}{s^{3r}t^{3l}} \left(\frac{x-A}{k}\right)^c \left(\frac{y-B}{j}\right)^d dsdt$$
$$+ \frac{1}{m} \int_{\beta B}^{y} \int_{\alpha A}^{x} \frac{-t(y-t)}{s^{3r}t^{3l}} \left(\frac{x-A}{k}\right)^c \left(\frac{y-B}{j}\right)^d dsdt$$

$$b_{\theta x3(x,y)}$$
$$= \frac{1}{m} \int_{y}^{B} \int_{x}^{A} \frac{(x-s)}{s^{3r}t^{3l}} (\frac{x-A}{k})^c (\frac{y-B}{j})^d dsdt$$

$$b_{\theta y3(x,y)}$$
$$= \frac{1}{m} \int_{y}^{B} \int_{x}^{A} \frac{(y-t)}{s^{3r}t^{3l}} (\frac{x-A}{k})^c (\frac{y-B}{j})^d dsdt$$

Node 4:

$$b_{w4(x,y)}$$
$$= \frac{1}{m} \int_{y}^{B} \int_{\alpha A}^{x} \frac{(A-s)(x-s)}{s^{3r}t^{3l}} \left(\frac{x-A}{k}\right)^c \left(\frac{y-B}{j}\right)^d dsdt$$
$$+ \frac{1}{m} \int_{\beta B}^{y} \int_{\alpha A}^{x} \frac{-t(y-t)}{s^{3r}t^{3l}} \left(\frac{x-A}{k}\right)^c \left(\frac{y-B}{j}\right)^d dsdt$$

$$b_{\theta x4(x,y)}$$
$$= \frac{1}{m} \int_{y}^{B} \int_{\alpha A}^{x} \frac{(x-s)}{s^{3r}t^{3l}} (\frac{x-A}{k})^c (\frac{y-B}{j})^d dsdt$$

$$b_{\theta y4(x,y)}$$
$$= \frac{1}{m} \int_{y}^{B} \int_{\alpha A}^{x} \frac{(y-t)}{s^{3r}t^{3l}} (\frac{x-A}{k})^c (\frac{y-B}{j})^d dsdt$$

where A: is the length, B: is the width of the plate, s and t: are integral variables, r and l: are thickness parameters, k and j: are stiffnesses (EI) in the x-direction and y-direction, c/d: is the inhomogeneous ratio in x and y directions (E_x/E_y and $c+d=1$. The following properties are assumed for the FGM plate:

$$h(x, y) = h_1 (\frac{x}{A})^r (\frac{y}{B})^l \text{ and } r \neq \frac{1}{3},1 , \; l \neq \frac{1}{3},1$$

$$c,d = \frac{1}{2}$$

m is defined as:

$$m = \frac{E_0 h_1^3 / A^{3r} B^{3l}}{12(1-v^2)} \tag{16}$$

Figure 4 shows the parameters of Eq. (15).

Thus, the equations could be rewritten as:

Node 1:

$$b_{w1(x,y)} = \frac{1}{m}\frac{x^2(x-k)^{-3r}}{(1-3r)(3-3r)}\frac{(2A-x)y(y-j)^{-3l}}{1-3l}$$
$$+\frac{1}{m}\frac{y^2(y-j)^{-3r}}{(1-3l)(3-3l)}\frac{(2B-y)x(x-k)^{-3r}}{1-3r}$$

$$b_{\theta x1(x,y)} = \frac{1}{m}\frac{x^2(x-k)^{-3r}}{(2-3r)(1-3r)}\frac{y(y-j)^{-3l}}{(1-3l)}$$

$$b_{\theta y1(x,y)} = \frac{1}{m}\frac{x(x-k)^{-3r}}{(1-3r)}\frac{y^2(y-j)^{-3l}}{(1-3l)(2-3l)}$$

Node 2:

$$b_{w2(x,y)} = \frac{1}{m}(A^{2-3r}\left(\frac{A}{3-3r}-\frac{x}{2-3r}\right)$$
$$+\frac{x^3(x-k)^{-3r}}{(3-3r)(2-3r)})\frac{y(y-j)^{-3l}}{(1-3l)}$$
$$+\frac{1}{m}\frac{y^2(y-j)^{-3r}}{(2-3l)}\left(\frac{B}{1-3l}-\frac{y}{3-3l}\right)$$
$$+\frac{A^{1-3r}-x^3(x-k)^{-3r}}{(1-3l)}$$

$$b_{\theta x2(x,y)} = \frac{1}{m}(A^{1-3r}\left(\frac{-A}{2-3r}+\frac{x}{1-3r}\right)$$
$$+\frac{x^2(x-k)^{-3r}}{(2-3r)(1-3r)})\frac{y(y-j)^{-3l}}{(1-3l)}$$

$$b_{\theta y2(x,y)} = \frac{1}{m}\frac{A^{1-3r}-x(x-k)^{-3r}}{(1-3r)}\frac{y^2(y-j)^{-3l}}{(1-3l)(2-3l)}$$

Node 3:

$$b_{w3(x,y)}$$
$$= \frac{1}{m}(A^{2-3r}\left(\frac{A}{3-3r}-\frac{x}{2-3r}\right)$$
$$+\frac{x^3(x-k)^{-3r}}{(3-3r)(2-3r)})\frac{B^{1-3l}y(y-j)^{-3l}}{(1-3l)}$$
$$+\frac{1}{m}(B^{2-3l}\left(\frac{B}{3-3l}-\frac{y}{2-3l}\right)$$
$$+\frac{y^3(y-j)^{-3r}}{(3-3l)(2-3l)})(\frac{A^{1-3r}-x^3(x-k)^{-3r}}{(1-3l)})$$

$$b_{\theta x3(x,y)}$$
$$= \frac{1}{m}(A^{1-3r}\left(\frac{-A}{2-3r}+\frac{x}{1-3r}\right)$$
$$-\frac{x^2(x-k)^{-3r}}{(2-3r)(1-3r)})\frac{B^{1-3l}-y(y-j)^{-3l}}{(1-3l)}$$

$$b_{\theta y3(x,y)} = \frac{1}{m}\frac{A^{1-3r}-x(x-k)^{-3r}}{(1-3r)}(B^{1-3l}(\frac{-B}{2-3l}$$
$$-\frac{y}{1-3l})\frac{y^2(y-j)^{-3l}}{(1-3l)(2-3l)})$$

Node 4:

$$b_{w4(x,y)}$$
$$= \frac{1}{m}(\frac{Ax^2(x-k)^{-3r}}{(1-3r)(2-3r)}$$
$$-\frac{x^3(x-k)^{-3r}}{(3-3r)(2-3r)})\frac{B^{1-3l}y(y-j)^{-3l}}{(1-3l)}$$
$$+\frac{1}{m}(B^{2-3l}\left(\frac{B}{3-3l}-\frac{y}{2-3l}\right)$$
$$+\frac{y^3(y-j)^{-3r}}{(3-3l)(2-3l)})(\frac{x(x-k)^{-3r}}{(1-3r)})$$

$$b_{\theta x4(x,y)} = \frac{1}{m}\frac{x^2(x-k)^{-3r}}{(2-3r)(1-3r)}\frac{B^{1-3l}-y(y-j)^{-3l}}{(1-3l)}$$

$$b_{\theta y4(x,y)} = \frac{1}{m}\frac{x^2(x-k)^{-3r}}{(1-3r)}(B^{1-3l}(\frac{-B}{2-3l}$$
$$-\frac{y}{1-3l})\frac{y^2(y-j)^{-3l}}{(1-3l)(2-3l)})$$

Considering a tapered FGM plate under transverse load $q(x,y)$, a two-determinate analysis can be used to calculate the support reactions, i.e. *C-C-F-F* plates (Figure 5). It can be written using the superposition principle:

$$\begin{Bmatrix} w_1 \\ \theta_{x1} \\ \theta_{y1} \end{Bmatrix}^{(a)} = \begin{Bmatrix} w_1 \\ \theta_{x1} \\ \theta_{y1} \end{Bmatrix}^{(b)} + \begin{Bmatrix} w_1 \\ \theta_{x1} \\ \theta_{y1} \end{Bmatrix}^{(c)} = 0 \qquad (17)$$
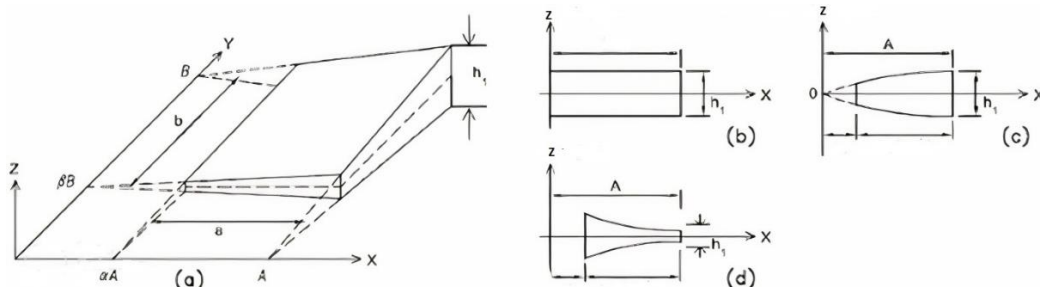
Fig. 4. Plate parameters: a) Three-dimensional view of the plate; b) Plate with fixed thickness; c) Plate with gradually increasing thickness; and d) Plate with gradually decreasing thickness
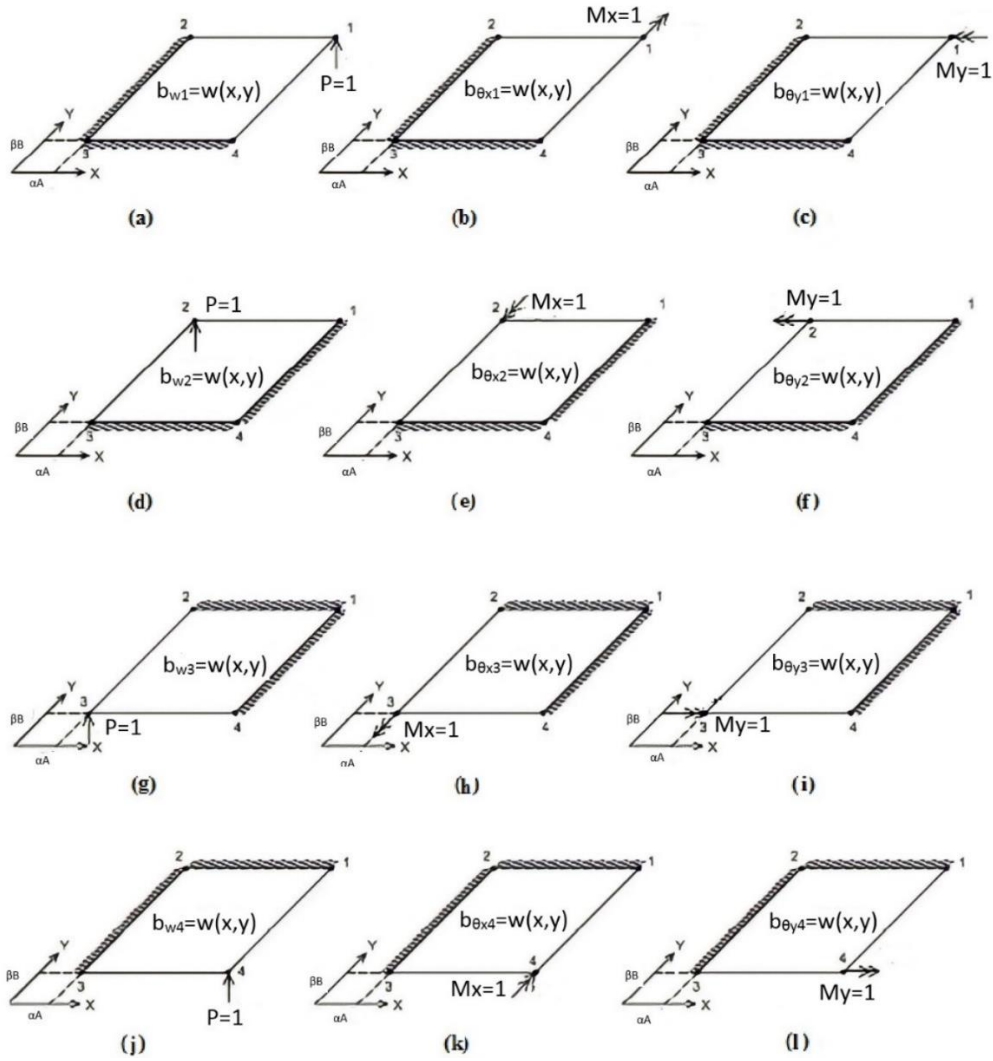
Fig. 5. Positive directions: a) Load acting at x, y causes a transverse displacement of Node 1; b) Unit load acting at x, y bends rotation of Node 1 in the x-direction; c) Unit load acting at x, y bends the rotation of Node 1 in the y-direction; d) Load acting at x, y causes a transverse displacement of Node 2; e) Unit load acting at x, y bends rotation of Node 2 in the x-direction; f) Unit load acting at x, y bends the rotation of Node 2 in the y-direction; g) Load acting at x, y causes a transverse displacement of Node 3; h) Unit load acting at x, y bends rotation of Node 3 in the x-direction; i) Unit load acting at x, y bends the rotation of Node 3 in the y-direction; j) Load acting at x, y causes a transverse displacement of Node 4; k) unit load acting at x, y bends rotation of Node 4 in the x-direction; and l) Unit load acting at x, y bends the rotation of Node 4 in the y-direction

in cases (a) - (c), w_1, θ_{x1}: stand for the nodal displacements at node i in Figures 5a-5c, respectively. BDFs can be used to measure nodal displacements at node 1:

$$\begin{Bmatrix} w_1 \\ \theta_{x1} \\ \theta_{y1} \end{Bmatrix}^{(b)} = \int\limits_{\beta B}^{B}\int\limits_{\alpha A}^{A} q_z(x,y) \begin{Bmatrix} b_{w1}(x,y) \\ b_{\theta x1}(x,y) \\ b_{\theta y1}(x,y) \end{Bmatrix} dxdy \quad (18)$$

$$\begin{Bmatrix} w_1 \\ \theta_{x1} \\ \theta_{y1} \end{Bmatrix}^{(c)} = F_{11} \begin{Bmatrix} F^1 \\ M_x^1 \\ M_y^1 \end{Bmatrix} \quad (19)$$

The matrix F_{11} represents the nodal flexibility of node 1 in Eq. (8). By using Eqs. (18) to (20), one obtains:

$$\begin{Bmatrix} F^1 \\ M_x^1 \\ M_y^1 \end{Bmatrix} = -F_{11}^{-1} \int\limits_{\beta B}^{B}\int\limits_{\alpha A}^{A} q_z(x,y) \begin{Bmatrix} b_{w1}(x,y) \\ b_{\theta x1}(x,y) \\ b_{\theta y1}(x,y) \end{Bmatrix} dxdy$$

(20)

in which F_{11}^{-1} is the nodal stiffness matrix of node 1. Similarly, other nodes also receive support reactions. Thus the support reactions of node i (i =1, .., 4) are:

$$\begin{Bmatrix} F^i \\ M_x^i \\ M_y^i \end{Bmatrix} = -F_{ii}^{-1} \int_{\beta B}^{B} \int_{\alpha A}^{A} q_z(x,y) \begin{Bmatrix} b_{wi}(x,y) \\ b_{\theta xi}(x,y) \\ b_{\theta yi}(x,y) \end{Bmatrix} dxdy \tag{21}$$

Support reactions with opposite signs have the same magnitude as nodal equivalent forces, so the vector F containing nodal equivalent forces is equal:

$$F = \sum \int_{\beta B}^{B} \int_{\alpha A}^{A} q_z(x,y) b dxdy \tag{22}$$

where $\sum$ and
$b = \begin{bmatrix} b_{w1} & b_{\theta x1} & b_{\theta y1} & b_{w2} & b_{\theta x2} & b_{\theta y2} & b_{w3} & b_{\theta x3} & b_{\theta y3} & b_{w4} & b_{\theta x4} & b_{\theta y4} \end{bmatrix}^T$
are the matrices indicating nodal stiffness and nodal BDFs for nodes 1 to 4.

Comparing Eq. (7) with Eq. (22), based on the BDFs, new shape functions are created:

$$N = b^T \sum \tag{23}$$

The stiffness matrices are determined by using Eq. (7) to Eq. (9). Any analysis should follow these steps. A program developed in MATLAB to do these steps automatically and make it practical and economical.

The shape function of Figure 5a is shown in MATLAB as an example in Figure 6. Based on Figure 6 the displacement of node 1 is the superposition of the three forces (P, M_x and M_y) that are calculated by this multiplication. In the case of rotation, the derivative is needed. The nodal stiffness matrix is evaluated after inverting the nodal flexibility matrix. Using a superposition of the shape functions, each edge's movement can be calculated.

FEM can calculate shapes such as circular, triangular, or trapezoidal by using rectangular elements. (Bramble and Zlámal, 1970). The examples of the other shapes are outside the scope of this paper.
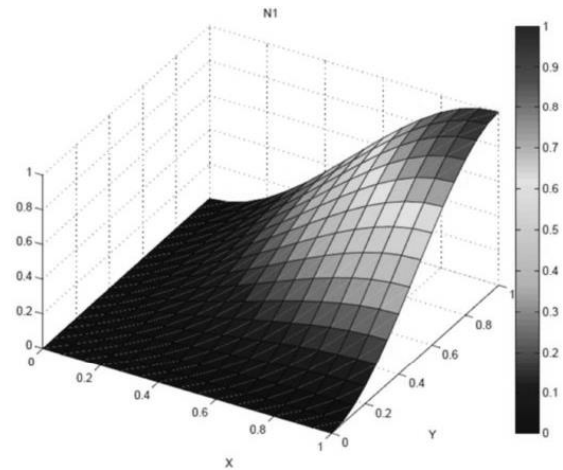
Fig. 6. First Shape function of Node 1

3. Results and Discussion

A step-by-step procedure is described below for performing a structural analysis of FGM plates using BDFs:

Step 1: Calculation of BDFs using Section 2.2.

Step 2: Matrix analysis of nodal flexibility using Eq. (15).

Step 3: Computation of $\sum$ using Eq. (22).

Step 4: Reaching the shape functions using Eq. (23).

Step 5: Formulation of stiffness matrices using Eq. (7) to Eq. (9).

Demonstrating the accuracy and applicability of 2D-DTM in free vibration analysis of Kirchhoff plate with in-plane functionally graded material, the following examples are given numerically as a validation test of the method. To achieve this, consider a rectangular in-plane FGM plate, with a length of a and a width of b, is shown in Figure 1. The material properties such as the elastic modulus E and mass density ρ are varying in-plane as mentioned in Section 2.1.

$$E = V_l E_l + V_r E_r \tag{24}$$

$$\rho = V_l \rho_l + V_r \rho_r \tag{25}$$

$$V_l + V_r = 1 \tag{26}$$

The most appropriate and simplest distribution of materials property is power-low distribution as follows

$$V_l = (y/b)^n \quad, \quad V_r = [1-(y/b)^n] \qquad (27)$$

where n: is the material graded index which is a real number such as 0, 0.5, 1, 2. Consequently, Eq. (24) and Eq. (25) can be represented as:

$$E = (y/b)^n E_l + [1-(y/b)^n] E_r \quad,$$
$$\rho = (y/b)^n \rho_l + [1-(y/b)^n] \rho_r \qquad (28)$$

Assuming the constant Poisson's ratio and substituting Eq. (28) in Eq. (24), Eq. (25) can be rewritten as follows, which is the general differential equation of the FGM plates, after replacing all parameters:

$$\frac{\partial^2}{\partial \xi^2} \left[-\frac{\left(\frac{y}{b}\right)^n E_1 + \left[1-\left(\frac{y}{b}\right)^n\right] E_r}{12(1-v^2)} hy^3 \left(b^4 \frac{\partial^2 w}{\partial \xi^2} \right.\right.$$
$$\left.\left. + va^2 b^2 \frac{\partial^2 w}{\partial \eta^2}\right)\right]$$
$$+2\frac{\partial^2}{\partial \xi \partial \eta} \left[-\frac{\left(\frac{y}{b}\right)^n E_1 + \left[1-\left(\frac{y}{b}\right)^n\right] E_r}{12(1-v^2)} hy^3 a^2 b^2 (1 \right.$$
$$\left. - v)\left(\frac{\partial^2 w}{\partial \xi \partial \eta}\right)\right]$$
$$+\frac{\partial^2}{\partial \eta^2} \left[-\frac{\left(\frac{y}{b}\right)^n E_1 + \left[1-\left(\frac{y}{b}\right)^n\right] E_r}{12(1-v^2)} hy^3 (a^4 \frac{\partial^2 w}{\partial \eta^2} \right.$$
$$\left. + va^2 b^2 \left(\frac{\partial^2 w}{\partial \xi^2}\right)\right]$$
$$+[\left(\frac{y}{b}\right)^n \rho_1 + \left[1-\left(\frac{y}{b}\right)^n\right]\rho_r] hwa^4 b^4 \omega^2$$
$$-\frac{\left(\frac{y}{b}\right)^n \rho_1 + \left[1-\left(\frac{y}{b}\right)^n\right]\rho_1}{12} h^3 \omega^2 \left(a^2 b^4 \frac{\partial^2 w}{\partial \xi^2} \right.$$
$$\left. + a^4 b^2 \frac{\partial^2 w}{\partial \eta^2}\right) = 0$$

$$(29)$$

The FGM plate considered here is made from ceramic and metal, in which the material is fully ceramic ($E_c = 7.65 \times 10^{10}$ P_a and $\rho_c = 2.5 \times 10^3$ kg/m³) at $y = 0 (\eta = 0)$ and fully metal ($E_m = 2.06 \times 10^{11}$ P_a and $\rho_m = 7.85 \times 10^3$ kg/m³) at $y = b (\eta = 1)$ and the constant Poisson's ratio is assumed as $v = 0.3$.

Considering different boundary conditions of the various edges of a square plate such as Simply supported (S), Clamped (C) and Free edge (F), the presented general procedure has been employed to calculate the first non-dimensional transverse natural frequency (Ω which is followed up $\Omega^2 = \omega l^2 \sqrt{\frac{h\rho_0}{D_0}}$ in which $D_0 = \frac{E_0}{12(1-v^2)} h^3$, $\rho_0 = \rho_c$ and $E_0 = E_c$) of the considered plate for different values of the n material graded index, and a, plate width. The results are shown in Tables 1-4 and compared with those reported by Liu et al. (2010). In these tables, all the plates are simply supported $x = 0$ and $x = a$ which are denoted by the two first letters. Similarly, the boundaries conditions at $y = 0$ and $y = b$ are shown by the third and fourth letters respectively. As it is demonstrated in the tables, the results have excellent agreement with those of Levy-type solution obtained by Liu et al. (2010). This close agreement clearly demonstrates the capability of the present general method in calculating the non-dimensional natural frequency of in-plane FGM plates. This general method can be applied for any other recursive formula which is obtained from the governing differential equation of the plate with arbitrary material and geometrical properties.

Table 1. The values of non-dimensional natural frequency Ω for different boundary conditions

n	Method	SSCS	SSCF	SSCC	SSSF	SSSC	SSSS	SSFS	SSFC	SSFF
					$a = 1$					
0	Differ. Eq.	4.863	3.562	5.381	3.418	4.863	4.443	3.418	3.562	3.104
	BDFs	4.863	3.563	5.380	3.419	4.863	4.443	3.417	3.562	3.103
0.5	Differ. Eq.	4.644	3.369	5.143	3.419	4.717	4.277	3.380	3.555	3.940
	BDFs	4.645	3.370	5.143	3.418	4.718	4.275	3.382	3.556	3.942
1	Differ. Eq.	4.641	3.349	5.199	3.243	4.777	4.306	3.433	3.624	3.016
	BDFs	4.643	3.348	5.202	3.245	4.780	4.307	3.432	3.623	3.016
2.5	Differ. Eq.	4.769	3.347	5.408	3.247	4.941	4.413	3.480	3.671	3.039
	BDFs	4.768	3.347	5.410	3.248	4.941	4.412	3.481	3.672	3.042

Table 2. The values of non-dimensional natural frequency Ω for different boundary conditions

n	Method	SSCS	SSCF	SSCC	SSSF	SSSC	SSSS	SSFS	SSFC	SSFF
					$\alpha = 5$					
0	Differ. Eq.	3.964	1.963	4.753	1.159	3.964	3.204	1.160	1.964	0.614
	BDFs	3.964	1.964	4.756	1.162	3.964	3.205	1.162	1.965	0.614
0.5	Differ. Eq.	3.707	1.727	4.531	1.160	3.894	3.095	1.178	2.097	0.595
	BDFs	3.706	1.730	4.533	1.160	3.893	3.095	1.178	2.097	0.595
1	Differ. Eq.	3.703	1.665	4.583	1.068	3.960	3.101	1.209	2.198	0.597
	BDFs	3.706	1.667	4.585	1.071	3.962	3.103	1.212	2.199	0.598
2.5	Differ. Eq.	3.801	1.652	4.806	1.059	4.112	3.139	1.230	2.246	0.602
	BDFs	3.803	1.584	4.805	1.062	4.113	3.141	1.229	2.246	0.603

Table 3. The values of non-dimensional natural frequency Ω for different boundary conditions

n	Method	SSCS	SSCF	SSCC	SSSF	SSSC	SSSS	SSFS	SSFC	SSFF
					$\alpha = 20$					
0	Differ. Eq.	3.929	1.881	4.732	0.562	3.929	3.146	0.568	1.881	0.153
	BDFs	3.930	1.883	4.735	0.563	3.930	3.146	0.568	1.882	0.153
0.5	Differ. Eq.	3.669	1.631	4.511	0.569	3.863	3.040	0.579	2.028	0.148
	BDFs	3.671	1.632	4.513	0.570	3.863	3.042	0.580	2.031	0.148
1	Differ. Eq.	3.665	1.562	4.562	0.522	3.929	3.045	0.595	2.133	0.149
	BDFs	3.667	1.565	4.565	0.523	3.930	3.046	0.596	2.136	0.149
2.5	Differ. Eq.	3.760	1.547	4.785	0.517	4.081	3.075	0.606	2.183	0.150
	BDFs	3.761	1.546	4.784	0.519	4.084	3.075	0.608	2.183	0.150

Table 4. The values of non-dimensional natural frequency Ω for different boundary conditions

n	Method	SSCS	SSCF	SSCC	SSSF	SSSC	SSSS	SSFS	SSFC	SSFF
					$\alpha = 1000$					
0	Differ. Eq.	3.926	1.875	4.730	0.080	3.927	3.142	0.080	1.875	0.003
	BDFs	3.927	1.875	4.730	0.080	3.927	3.142	0.080	1.875	0.003
0.5	Differ. Eq.	3.666	1.624	4.509	0.080	3.861	3.036	0.082	2.023	0.003
	BDFs	3.666	1.626	4.510	0.080	3.862	3.036	0.082	2.024	0.003
1	Differ. Eq.	3.662	1.555	4.561	0.074	3.927	3.041	0.084	2.129	0.003
	BDFs	3.663	1.556	4.561	0.074	3.927	3.042	0.084	2.129	0.003
2.5	Differ. Eq.	3.757	1.539	4.784	0.073	4.078	3.071	0.086	2.178	0.003
	BDFs	3.757	1.539	4.785	0.073	4.078	3.071	0.086	2.179	0.003

For testing, results are compared to those of Liu et al. (2010) shown in Table 1 to Table 4. Nevertheless, new results had to be presented that had not been computed before. For this reason, the added boundary conditions CCFF and CCCC which were not shown in Liu et al. (2010) are calculated in this research.

The results in this paper confirm that the free vibrations of the FGM plate match the homogeny plate in specific N_s. This is the frequency that equals that of the homogeny plate. This can be useful for replacing some cheaper material in the specific Ω_0, if it is needed. The results of the N_s, for several cases, are shown in Table 7.

Another important issue is convergence. Figures 7 and 8 show how many elements are needed in FEM in order to arrive at the answer for $n = 1$ and 2.5, respectively. For both of them, α is equal to one and they are in SSSS condition. Upon selecting 48 elements, the graph begins to converge to the answer after a dramatic growth while in $n = 2.5$, a fracturing can be observed.

The graph of Ω based on α is represented in Figure 9. It shows a significant drop in the frequency before $\alpha = 5$ but a slight decrease after that.

Table 5. The values of non-dimensional natural frequency Ω for different CCFFs

CCFF				α	
n		1	5	20	1000
0	BDFs	3.136	2.786	2.757	2.692
0.5	BDFs	2.997	2.640	2.629	2.566
1	BDFs	3.030	2.671	2.658	2.596
2.5	BDFs	3.125	2.791	2.748	2.682

Table 6. The values of non-dimensional natural frequency Ω for different CCCCs

CCCC		α			
n		1	5	20	1000
0	BDFs	8.021	6.915	6.896	6.611
0.5	BDFs	7.781	6.854	6.825	6.492
1	BDFs	7.866	6.934	6.902	6.576
2.5	BDFs	8.282	7.921	7.639	7.388

Table 7. The values of N_s for different boundary conditions

N_s	Boundary Conditions (BCs)					
α	SSCS	SSCC	SSSC	SSSS	CCCC	CCFF
1	3.64	2.28	1.77	2.94	1.55	2.67
5	5.19	2.14	1.02	5.02	0.97	2.43
20	5.17	2.16	1	6.17	0.98	2.65
1000	5.17	2.13	1	6.17	1.08	2.67
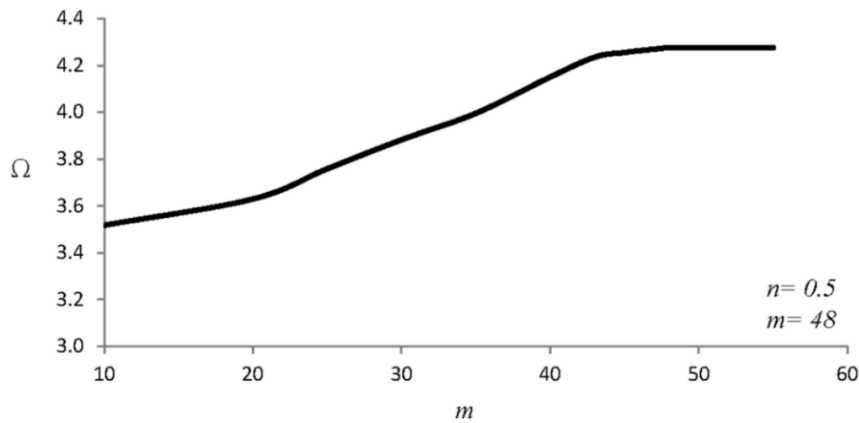
Fig. 7. Convergence of frequency for $\alpha = 1$, n = 0.5 and SSSS condition
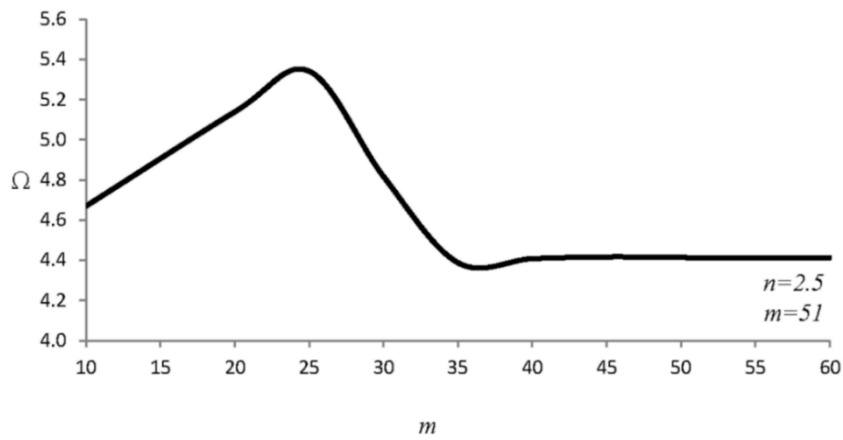
Fig. 8. Convergence of frequency for $\alpha = 1$, n = 2.5 and SSSS condition
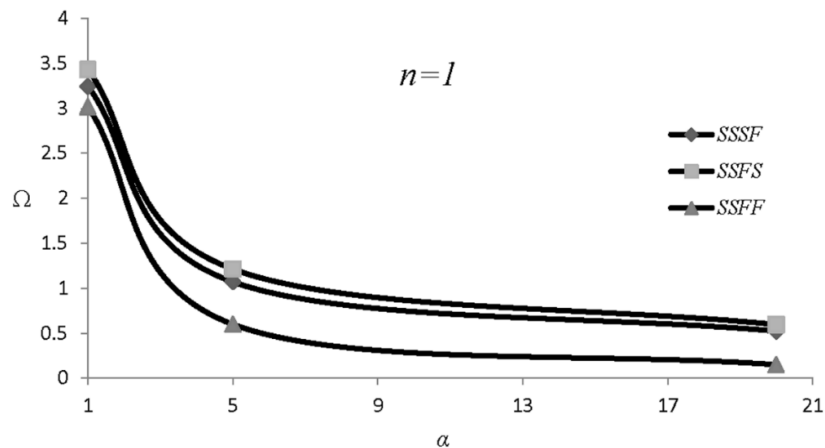
Fig. 9. The impact of α on Ω

4. Conclusions

Using the Finite Element Method (FEM) and Basic Displacement Functions (BDFs), this paper presented an efficient element for in-plane Functionally Graded Materials (FGMs) plates vibration analysis. The first step was to define and generate BDFs. New shape functions could be derived mechanically by expressing them as derived BDFs. Furthermore, the Finite Element method was used to compute the structural stiffness and the mass matrix of the considered beams. This method was tested on several numerical examples, which showed excellent agreement with the literature with regard to accuracy and economy. Several examples demonstrated that the method is super-convergent for either free vibration or bent beams with different boundary conditions.

The following benefits can be attributed to this method:
- Through the presented method, any variations in the taper ratio and mechanical properties of the plate can be incorporated into the design.
- The generality of stiffness methods and the accuracy of forces methods are combined to create a new element.
- Implementing the new element, free vibration analyses are performed with lower elements. As a result, the time and cost of the analyses are significantly reduced.

Different structural applications have proven the concept of BDFs' competency. In order to facilitate the study of these other complex structural elements as well as the application of BDFs and other advanced materials, such as functionally graded materials (FGMs), the authors are extending BDFs to shells.

5. Symbol List

a	length of the plate along x direction
b	length of the plate along y direction
b	vector of BDFs
E	modulus of elasticity
F	vector of nodal forces
F_{ii}	nodal flexibility matrices of ith node
$h(x_j, y_j)$	thickness of the plate at point j (x_j, y_j)
K	stiffness matrix
M	mass matrix
N	vector of shape functions
N_s	special material graded-index
$q_z(x,y)$	external transverse load
r	taper factor of the plate in x direction
s	taper factor of the plate in y direction
w	transverse displacement
w_0	the displacement function
x, y	longitudinal coordinates along plate
θ	angle of rotation
Σ	matrix containing nodal stiffness matrices
Ω	non-dimensional Eigen frequency
ω	Eigen frequency

6. References

Attarnejad, R., Semnani, S.J. and Shahba, A. (2010). "Basic displacement functions for free vibration analysis of non-prismatic Timoshenko beams", *Finite Elements in Analysis and Design*, 46(10), 916-929, https://doi.org/10.1016/j.finel.2010.06.005.

Bacciocchi, M., Eisenberger, M., Fantuzzi, N., Tornabene, F. and Viola, E. (2016). "Vibration analysis of variable thickness plates and shells by the generalized differential quadrature method", *Composite Structures*, 156, 218-237, https://doi.org/10.1016/j.compstruct.2015.12.004.

Bramble, J. H. and Zlámal, M. (1970). "Triangular elements in the finite element method", *Mathematics of Computation*, 24(112), 809-820, https://doi.org/10.1090/S0025-5718-1970-0282540-0.

Cheng, Z.Q. and Batra, R.C. (2000). "Three-dimensional thermoelastic deformations of a functionally graded elliptic plate", *Composites Part B: Engineering*, 31(2), 97-106, https://doi.org/10.1016/S1359-8368(99)00069-4.

Chiba, R. (2019). "Natural convection analysis of water near its density extremum between finite vertical plates: A differential transform

approach", *International Journal of Mathematical Modelling and Numerical Optimisation*, 9(4), 429-448, https://doi.org/10.1504/IJMMNO.2019.102601.

Das, R.R. (2010). "Adhesion failure and delamination of bonded tubular joints made with laminated FRP composites and functionally graded materials", Doctoral Dissertation, IIT Kharagpur, http://dx.doi.org/10.1016/j.compstruct.2020.113386.

Fallah, F. and Karimi, M. (2019). "Non-linear analysis of functionally graded sector [lates with simply supported radial edges under transverse loading", *Mechanics of Advanced Composite Structures*, 6(1), 65-74, https://doi.org/10.22075/macs.2019.16171.116.

Fallah, N., Parayandeh-Shahrestany, A. and Golkoubi, H. (2017). "A Finite Volume formulation for the elasto-plastic analysis of rectangular Mindlin-Reissner plates, a non-layered approach", *Civil Engineering Infrastructures Journal*, 50(2), 293-310, https://doi.org/ 10.7508/ceij.2017.02.006.

Goupee, A.J. and Vel, S.S. (2006). "Optimization of natural frequencies of bidirectional functionally graded beams", *Structural and Multidisciplinary Optimization*, 32(6), 473-484, https://doi.org/10.1007/s00158-006-0022-1.

Gupta, A. (2020). "Functionally graded structures: Design and analysis of tailored advanced composites", In *Characterization, Testing, Measurement, and Metrology,* (pp. 33-55), CRC Press.

Hadji, L., Zouatnia, N. and Bernard, F. (2019). "An analytical solution for bending and free vibration responses of functionally graded beams with porosities: Effect of the micromechanical models", *Structural Engineering and Mechanics*, 69(2), 231-241, https://doi.org/10.12989/sem.2019.69.2.231.

Hamrit, F. and Necib, B. (2018). "Analysis of mechanical structures using plate finite element method under different boundary conditions", *Diagnostyka*, 19(2), 3-9, http://dx.doi.org/10.29354/diag/86257.

Kaplunov, J., Erbas, B. and Ege, N. (2021). "An asymptotic theory for a functionally graded plate", *BGSIAM'21*, 32, Bulgaria.

Kumar, V., Singh, S.J., Saran, V.H. and Harsha, S.P. (2021). "Vibration characteristics of porous FGM plate with variable thickness resting on Pasternak's foundation", *European Journal of Mechanics-A/Solids*, 85(1 January), 104124, https://doi.org/10.1016/j.euromechsol.2020.104124.

Kumar, Y. (2018). "The Rayleigh–Ritz method for linear dynamic, static and buckling behavior of beams, shells and plates: A literature review", *Journal of Vibration and*

Control, 24(7), 1205-1227, https://doi.org/10.1177/1077546317694724.

Lal, R. and Saini, R. (2020). "Vibration analysis of FGM circular plates under non-linear temperature variation using generalized differential quadrature rule", *Applied Acoustics*, 158(15 January), 107027, https://doi.org/10.1016/j.apacoust.2019.107027.

Leissa, A.W. (1969). "Vibration of plates", Washington: NASA SP-160, US Government Printing Office,

Liu, D.Y., Wang, C.Y. and Chen, W.Q. (2010). "Free vibration of FGM plates with in-plane material inhomogeneity", *Composite Structures*, 92(5), 1047-1051, https://doi.org/10.1016/j.compstruct.2009.10.001.

Liu, Y.Y., Shu, C., Zhang, H.W., Yang, L.M. and Lee, C. (2021). "An efficient high-order least square-based finite difference-finite volume method for solution of compressible Navier-Stokes equations on unstructured grids", *Computers and Fluids*, 222(30 May), 104926, https://doi.org/10.1016/j.compfluid.2021.104926.

Makvandi, H., Moradi, S., Poorveis, D. and Heidari Shirazi, K. (2019). "Crack identification in postbuckled plates using differential quadrature element method and sequential quadratic programming", *Amirkabir Journal of Mechanical Engineering*, 51(3), 51-60, https://doi.org/10.22060/mej.2018.13543.5660.

Malekzadeh, P., Setoodeh, A.R. and Shojaee, M. (2018). "Vibration of FG-GPLs eccentric annular plates embedded in piezoelectric layers using a transformed differential quadrature method", *Computer Methods in Applied Mechanics and Engineering*, 340(1 October), 451-479, https://doi.org/10.1016/j.cma.2018.06.006.

Miyamoto, Y., Kaysser, W.A., Rabin, B.H., Kawasaki, A. and Ford, R.G. (Eds.). (2013). *Functionally graded materials: design, processing and applications,* Vol. 5, Springer Science & Business Media.

Mora, P., Ducasse, E. and Deschamps, M. (2016). "Interaction of guided waves with cracks in an embedded multilayered anisotropic plate by using a Boundary Element approach"*, Physics Procedia,* 70, 326-329, https://doi.org/10.1016/j.phpro.2015.08.217.

Naumenko, K. and Eremeyev, V.A. (2017). "A layer-wise theory of shallow shells with thin soft core for laminated glass and photovoltaic applications", *Composite Structures*, 178, 434-446, https://doi.org/10.1016/j.compstruct.2017.07.007.

Njim, E.K., Al-Waily, M. and Bakhy, S.H. (2021).

"A critical review of recent research of free vibration and stability of functionally graded materials of sandwich plate", In *IOP Conference Series: Materials Science and Engineering,* Vol. 1094, No. 1, p. 012081, IOP Publishing, https://doi.org/10.1088/1757-899x/1094/1/012081.

Pachenari, Z. and Attarnejad, R. (2014a). "Free vibration of tapered Mindlin plates using basic displacement functions", *Arabian Journal for Science and Engineering*, 39(6), 4433-4449, https://doi.org/10.1007/s13369-014-1071-1.

Pachenari, Z. and Attarnejad, R. (2014b). "Analysis of tapered thin plates using basic displacement functions", *Arabian Journal for Science and Engineering*, 39(12), 8691-8708, https://doi.org/10.1007/s13369-014-1407-x.

Ramkumar, R.L., Chen, P.C. and Sanders, W.J. (1987). "Free vibration solution for clamped orthotropic plates using Lagrangian multiplier technique", *AIAA Journal*, 25(1), 146-151, https://doi.org/10.2514/3.9594.

Reddy, J. (2000). "Analysis of functionally graded plates" *International Journal for Numerical Methods in Engineering*, 47(1-3), 663-684, https://doi.org/10.1002/(SICI)1097-0207(20000110/30)47:1/3%3C663::AID-NME787%3E3.0.CO;2-8.

Saidi, H. and Sahla, M. (2019). "Vibration analysis of functionally graded plates with porosity composed of a mixture of Aluminum (Al) and Alumina (Al_2O_3) embedded in an elastic medium", *Frattura ed Integrità Strutturale*, 13(50), 286-299, https://doi.org/10.3221/IGF-ESIS.50.24.

Shahir, H. and Delfan, S. (2021). "Numerical investigation of nailing pattern effect on nailed wall performance", *Civil Engineering Infrastructures Journal*, 54(2), 331-350, https://doi.org/10.22059/ceij.2021.298632.1659.

Şimşek, M. (2016). "Buckling of Timoshenko beams composed of two-dimensional functionally graded material (2D-FGM) having different boundary conditions", *Composite Structures*, 149(1 August), 304-314, https://doi.org/10.1016/j.compstruct.2016.04.034.

Szilard, R. (2004). "Theories and applications of plate analysis: Classical, numerical and engineering methods", *Applied Mechanics Reviews*, 57(6), B32-B33, https://doi.org/10.1115/1.1849175.

Teimouri, H., Davoodi, M.R., Mostafavian, S.A. and Khanmohammadi, L. (2021). "Damage detection in double layer grids with modal strain energy method and Dempster-Shafer theory", *Civil Engineering Infrastructures Journal*, 54(2), 253-266, https://doi.org/10.22059/ceij.2020.294512.1644.

Tenenbaum, J., Deutsch, A. and Eisenberger, M.

(2020). "Analytical buckling loads for rectangular orthotropic and symmetrically laminated plates", *AIAA Journal*, 58(2), 907-917, https://doi.org/10.2514/1.J058536.

Van Vinh, P., Dung, N.T. and Tho, N.C. (2021, February). "Modified single variable shear deformation plate theory for free vibration analysis of rectangular FGM plates", *Structures,* 29(1 February), 1435-1444, https://doi.org/10.1016/j.istruc.2020.12.027.

Vatani Oskouei, A. and Kiakojouri, F. (2015). "Non-linear dynamic analysis of steel hollow I-core sandwich panel under air blast loading", *Civil Engineering Infrastructures Journal*, 48(2), 323-344, https://doi.org/10.7508/ceij.2015.02.008.

Vidal, P., Gallimard, L., Polit, O. and Valot, E. (2021). "Analysis of functionally graded plates based on a variable separation method", *Mechanics of Advanced Materials and Structures*, 29(26), 4890-4901, https://doi.org/10.1080/15376494.2021.1942597.

Wang, X., Liang, X. and Jin, C. (2017). "Accurate dynamic analysis of functionally graded beams under a moving point load", *Mechanics Based Design of Structures and Machines*, 45(1), 76-91, https://doi.org/10.1080/15397734.2016.1145060.

Zakeri, M., Modarakar Haghighi, A. and Attarnejad, R. (2016). "On the analysis of FGM beams: FEM with innovative element", *Journal of Solid Mechanics*, 8(2), 348-364, https://dorl.net/dor/20.1001.1.20083505.2016.8.2.9.9.